This article has been accepted for inclusion in a future issue of this journal. Content is final as presented, with the exception of pagination.

Damped Harmonic Smoother for Trajectory Planning and Vibration Suppression

Luigi Biagiotti, Claudio Melchiorri, and Lorenzo Moriello

***Abstract*— In this brief, a novel filter for online trajectory generation is presented. The filter can be categorized as an input smoother since it acts on the input signal by increasing its continuity level. When fed with simple signals, as, e.g., a step input, it behaves like a trajectory generator that produces harmonic motions. Moreover, it can be combined with other filters, and in particular, with smoothers having a rectangular impulse response, in order to generate (online) more complex trajectories compliant with several kinematic constraints. On the other hand, being a filter, it possesses the capability of shaping the frequency spectrum of the output signal. This possibility can be profitably exploited to suppress residual vibration by imposing that the zeros of the filter cancel the oscillatory dynamics of the plant. For this purpose, the standard harmonic filter has been generalized in order to consider not only the natural frequency but also the damping coefficient of the plant. In this manner, the so-called "damped harmonic filter" and the related "damped harmonic trajectory" have been defined. By means of theoretical considerations, supported by experimental tests, the novel approach has been compared with the existing methods, and the advantages of its use have been proved.**

***Index Terms*— Harmonic trajectory, input shaping, residual vibration, smoother, trajectory planning.**

I. Introduction

THE growing interest for planning trajectories online has led to the development of a number of filters able to produce motion profiles with the desired degree of smoothness simply starting from basic reference signals to set the desired final position, such as step functions. For this purpose, many strategies have been proposed, including filtering and smoothing techniques by means of various kind of filters, ranging from finite impulse response filters [1]–[3] to inverse dynamics of the plant, or feedback control of a chain of integrators with bounds on velocity, acceleration, jerk, and so on, as, e.g., in [4]–[7]. In these latter works, time-optimal trajectory planners are proposed based on a closed-loop chain of integrators (whose output represents the desired trajectory) properly designed to track in the fastest possible way the reference input while remaining compliant with the given constraints. In [8], it is shown that time-optimal multisegment polynomial trajectories with constraints on the first n derivatives are equivalent to the outputs of a chain of n moving average filters, also known as rectangular smoothers (see Section II for a brief overview). On the other hand, in many contributions, mainly focused on a trajectory design via analytic expression optimization, the adoption of trigonometric functions is proposed with the purpose of planning motions with smoother acceleration or jerk profiles that reduce residual vibrations when applied to resonant systems (see [9]). In particular, in [10], polynomial multisegment trajectories (with constant jerk) and multisegment trajectories with square sine jerk have been experimentally compared in this respect, showing that the sine-based trajectories outperform the standard constant-jerk trajectories at the price of a noticeable increase of the motion duration.

The use of trigonometric functions has also been investigated in the input shaping framework, where filters similar—but not identical—to the one studied in this brief have been presented formerly (see [11]–[14]). However, these works only focus on the problem of residual vibration suppression, while a thorough analysis of the motion profiles obtained when used alone or with other filters has not been performed.

In this brief, we start from the results presented in the conference papers [15], [16], concerning the generation of trajectories by means of dynamic filters with trigonometric (and in particular sinusoidal) velocity, acceleration, or jerk profiles. These results are summarized in Sections II and III. Then, in Section IV, it has been shown that the main advantages of sinusoidal filters consist in the reduction of residual vibrations, since kinematic constraints can be more profitably satisfied with the use of rectangular smoothers. For this reason, a deep analysis of the performance achievable in vibrations suppression with this type of filter has been carried out, along with a comparison with some well-settled techniques available in the literature that involve the same motion duration. In this manner, the pros and cons of the use of sinusoidal motion profiles have been definitely proved. And, more importantly, in order to improve its performance, the harmonic smoother has been generalized, considering not only the natural frequency of the resonant plant but also its damping ratio. In this way, in Section V, the *"damped harmonic smoother"* and the novel *"damped harmonic trajectory"* have been defined. Finally, in Section VI, the experimental tests performed with the proposed filter are reported, and the achieved results have been summarized in Section VII.

II. Multisegment Trajectories and Smoothers

In [8], it has been shown that a multisegment trajectory $q_n(t)$ of order n, i.e., a trajectory with the first n derivatives bounded

Manuscript received July 31, 2018; revised October 11, 2018; accepted November 13, 2018. Manuscript received in final form November 15, 2018. Recommended by Associate Editor P. F. F. Odgaard. *(Corresponding author: Luigi Biagiotti.)*

L. Biagiotti is with the Department of Engineering "Enzo Ferrari," University of Modena and Reggio Emilia, 41125 Modena, Italy (e-mail: luigi.biagiotti@unimore.it).

C. Melchiorri and L. Moriello are with the Department of Electrical, Electronic and Information Engineering "Guglielmo Marconi," University of Bologna, 40136 Bologna, Italy (e-mail: claudio.melchiorri@unibo.it; lorenzo.moriello@unibo.it).

Color versions of one or more of the figures in this paper are available online at http://ieeexplore.ieee.org.

Digital Object Identifier 10.1109/TCST.2018.2882340

1063-6536 © 2018 IEEE. Personal use is permitted, but republication/redistribution requires IEEE permission.
See http://www.ieee.org/publications_standards/publications/rights/index.html for more information.

This article has been accepted for inclusion in a future issue of this journal. Content is final as presented, with the exception of pagination.

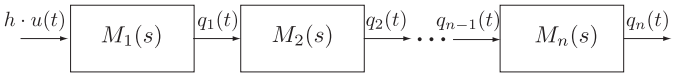

Fig. 1. System composed by n filters for the computation of an optimal trajectory of class $\mathcal{C}^{n-1}$.

(and, in particular, compliant with the symmetric constraints $q_{\min}^{(i)} = -q_{\max}^{(i)}$, $i = 1, \ldots, n$), can be obtained by filtering a step input with a cascade of n dynamic filters (see Fig. 1), each one characterized by the transfer function

$$M_i(s) = \frac{1}{T_i}\frac{1 - e^{-sT_i}}{s} \quad i = 1, \ldots, n \tag{1}$$

where the parameter T_i (in general, different for each filter) is a time length. As described in [8], the resulting trajectory $q_n(t)$ is composed of several polynomial segments $q_{n,k}(t)$ defined as a linear combination of the basis functions t^i, $i = 0, \ldots, n$, i.e., the kth segment is defined as $q_{n,k}(t) = \sum_{i=0}^{n} a_{i,k} t^i$.

The smoothness of the trajectory, that is the number of continuous derivatives, is strictly tied to the number of filters composing the chain. If n filters are considered, the resulting trajectory will be of class $\mathcal{C}^{n-1}$. For this reason, the filters (1) are also called *smoothers* since they increase the smoothness of the input signal, while the name *"rectangular*," used to denotes $M_i(s)$, refers to the shape of their impulse response.

The generic jth derivative $q_n^{(j)}(t)$ of the output trajectory is composed of polynomial functions, which are the linear combination of t^i, $i = 0, \ldots, n - j$, and accordingly, the nth derivative $q_n^{(n)}(t)$ is composed of constant tracts. For instance, the classical constant-jerk trajectory is obtained with three smoothers $M_i(s)$. Note that by increasing the smoothness of the trajectory adding extra filters in the chain, its duration augments as well. As a matter of fact, the total duration of a trajectory generated in this manner is simply given by the sum of the lengths of the impulse response of each filter, i.e., $T_{tot} = T_1 + T_2 + \cdots + T_n$. With the purpose of imposing desired bounds on velocity, acceleration, jerk, and higher derivatives, given a desired displacement h, the parameters T_i are set as

$$T_1 = \frac{|h|}{q_{\max}^{(1)}} \quad \text{and } T_i = \frac{q_{\max}^{(i-1)}}{q_{\max}^{(i)}}, \quad i = 2, \ldots, n \tag{2}$$

with the constraints

$$T_k \geq \sum_{i=k+1}^{n} T_i, \quad k = 1, \ldots, n-1. \tag{3}$$

Inequalities (3) are necessary and sufficient conditions for assuring the time optimality of the output trajectory and the compliance with the bounds $q_{\max}^{(i)}$, $i = 1, \ldots, n$. For more details, refer to [8].

Alternatively, the parameter T_i of each filter of the chain can be determined with the purpose of properly shaping its frequency response. As a matter of fact, the magnitude of the frequency response of a generic filter $M_i(j\omega)$ is

$$|M_i(j\omega)| = \left| \frac{\sin\left(\frac{\omega T_i}{2}\right)}{\frac{\omega T_i}{2}} \right| = \left| \operatorname{sinc}\left(\frac{\omega}{\omega_i}\right) \right|$$

where $\operatorname{sinc}(\cdot)$ denotes the normalized sinc function defined as $\operatorname{sinc}(x) = (\sin(\pi x)/\pi x)$ and $\omega_i = (2\pi/T_i)$. Note that function $|M_i(j\omega)|$ has a low-pass characteristic and is equal to zero for $\omega = k\,\omega_i$.

III. Sinusoidal Smoothers for the Generation of Multisegment Trajectories

The step response of the trajectory generator obtained by inserting, in the chain of n rectangular smoothers of Fig. 1, m filters characterized by the impulse response

$$s_i(t) = \begin{cases} \dfrac{\pi}{2T_i} \sin\left(\dfrac{\pi}{T_i} t\right), & \text{if } 0 \leq t \leq T_i \\ 0 & \text{otherwise} \end{cases} \tag{4}$$

is a multisegment trajectory, in which each tract is linear combinations of the basis functions t^i, $i = 0, \ldots, n$ and $\sin((\pi/T_j)t + \varphi_j)$, $j = 1, \ldots, m$, where φ_j are proper constants and it is supposed that all the parameters T_j are distinct. The transfer function of the filters can be readily obtained by Laplace transforming (4)

$$S_i(s) = \frac{1}{2}\left(\frac{\pi}{T_i}\right)^2 \frac{1 + e^{-sT_i}}{s^2 + \left(\frac{\pi}{T_i}\right)^2}. \tag{5}$$

Since the impulse response of $S_i(s)$ is described by a sine function, the filter is called *sinusoidal smoother*. Each sinusoidal smoother increases of two the continuity level of the output signal with respect to the input, and therefore, a generic trajectory generator based on n filters $M_i(s)$ and m filters $S_i(s)$ produces trajectories that are at least of class $\mathcal{C}^{n+2m-1}$.

For instance, if a step input of amplitude h is applied to a trajectory generator composed of a single sinusoidal smoother, the standard *harmonic trajectory* is obtained

$$q_h(t) = \mathcal{L}^{-1}\left\{ S_1(s)\frac{h}{s} \right\} = q_0 + \frac{h}{2}\left(1 - \cos\left(\frac{\pi}{T_1} t\right)\right)$$

where q_0 is the initial position and T_1 is the duration of the trajectory. For this reason, $S_i(s)$ is also called *"harmonic filter*." The harmonic trajectory $q_h(t)$ is of class $\mathcal{C}^1$, being the step is a discontinuous function, i.e., of class $\mathcal{C}^{-1}$.

More, in general, it is possible to obtain trajectories characterized by velocity, acceleration, jerk, or higher derivatives, depending on the order of the trajectory, composed only of sinusoidal functions by adding the sinusoidal filter $S_1(s)$ at the end of a chain of n filters $M_i(s)$. For instance, the profile $q_{1,h}(t)$ obtained with one rectangular filter and one sinusoidal filter is the *modified trapezoidal velocity* of class $\mathcal{C}^2$, while $q_{2,h}(t)$ generated by means of the cascade of two rectangular filters and one sinusoidal filter is the *modified double-S velocity* of class $\mathcal{C}^3$ (see Fig. 2). Also, in this case, the time optimality of the trajectory subject to kinematic constraints is guaranteed only if the time constants T_i of all the filters, including the harmonic smoother, satisfy the condition (3).

Note that the analytical expressions of composite trajectories $q_{n,h}(t)$ tend to become very complex and may be intractable even for small values of n, e.g., for $q_{2,h}(t)$, which is characterized by seven different tracts. In these cases,

This article has been accepted for inclusion in a future issue of this journal. Content is final as presented, with the exception of pagination.

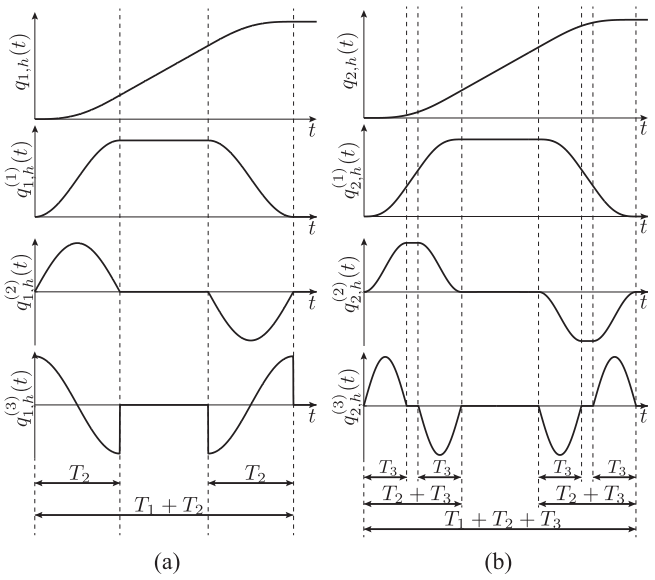

Fig. 2. Position, velocity, and acceleration profiles of (a) modified trapezoidal velocity trajectory $q_{1,h}$ and (b) modified double-S velocity trajectory $q_{2,h}$.

the filters, which are suitable for the online computation of the trajectory, are also preferable for off-line generation.

Considering that the filter $S_1(s)$ increases the continuity level of the trajectory $q_n(t)$ by two, the time constant T_{n+1} can be computed by taking into account the constraints on the $(n+1)$th and $(n+2)$th derivatives of the trajectory by assuming

$$T_{n+1} = \max\left\{\frac{\pi}{2}\frac{q^{(n)}_{\max}}{q^{(n+1)}_{\max}}, \sqrt{\frac{\pi^2}{2}\frac{q^{(n)}_{\max}}{q^{(n+2)}_{\max}}}\right\}. \tag{6}$$

Remark: The additional duration T_{n+1} caused by the sinusoidal filter, computed according to (6), is certainly higher than the duration of a cascade of two rectangular filters designed according the same constraints, i.e.,

$$T_{n+1} + T_{n+2} = \frac{q^{(n)}_{\max}}{q^{(n+1)}_{\max}} + \frac{q^{(n+1)}_{\max}}{q^{(n+2)}_{\max}}.$$

For this reason, when a task imposes only kinematic constraints, the use of rectangular filters $M_i(s)$ only is preferable, while sinusoidal smoothers can be helpful to fulfill different requirements, such as the suppression of residual vibrations.

IV. Vibrations Suppression With Sinusoidal Filters

In order to evaluate the capabilities of the sinusoidal filter in canceling residual vibrations, the motion system of Fig. 3, already considered in [8], has been assumed as a benchmark. It is composed of two inertias with a lightly damped elastic transmission. An ideal control system is supposed to impose the desired motion profile to the (rotor) inertia J_m, that is $q_m(t) = q_{\text{ref}}(t)$, being $q_{\text{ref}}(t)$ the reference trajectory obtained with the proposed filter. In this case, the dynamic relation between the reference trajectory $q_{\text{ref}}(t)$ and the tracking error

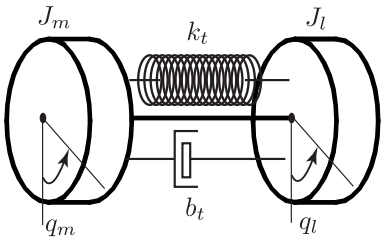

$$G(s) = \frac{2\delta\omega_n s + \omega_n^2}{s^2 + 2\delta\omega_n s + \omega_n^2}$$

$$\omega_n = \sqrt{\frac{k_t}{J_l}}, \quad \delta = \frac{b_t}{2\sqrt{k_t J_l}}$$

Fig. 3. Lumped constant model of a motion system with elastic transmission and transfer function $G(s) = (Q_l(s)/Q_m(s))$ between the motor position q_m and the load position q_l.

$\varepsilon(t) = q_l(t) - q_{\text{ref}}(t) = q_l(t) - q_m(t)$ is

$$\frac{E(s)}{Q_{\text{ref}}(s)} = \frac{-s^2}{s^2 + 2\delta\omega_n s + \omega_n^2} = G_\varepsilon(s) \tag{7}$$

where $E(s) = \mathcal{L}\{\varepsilon(t)\}$ and $Q_{\text{ref}}(s) = \mathcal{L}\{q_{\text{ref}}(t)\}$. Note that the tracking error $\varepsilon(t)$ at the end of the reference trajectory coincides with the definition of residual vibration [17].

It is possible to prove that when the plant is fully undamped, i.e., $\delta = 0$, the residual vibration is completely suppressed by a sinusoidal smoother $S_i(s)$, inserted in the chain of filters for reference generation, if

$$T_i = \frac{3}{2}\frac{2\pi}{\hat{\omega}_n} = \frac{3}{2}\hat{T}_0 \tag{8}$$

where $\hat{\omega}_n$ denotes the nominal value of the natural frequency of the plant and $\hat{T}_0$ is the (nominal value of the) period of the free oscillation. Since the magnitude of frequency response of the sinusoidal smoother is

$$|S_i(j\omega)| = \frac{\left|\cos\left(\pi\frac{\omega}{\omega_i}\right)\right|}{\left|1 - \left(\frac{\omega}{\omega_i/2}\right)^2\right|} \quad \text{with } \omega_i = \frac{2\pi}{T_i}$$

the condition (8) assures that $|S_i(j\hat{\omega}_n)| = 0$ and, accordingly, the oscillating component at the resonant frequency $\omega_r = \hat{\omega}_n$ is completely canceled. It is worth noting that the function $|S_i(j\omega_n)|$ represents the sensitivity of the filter in residual vibration suppression to the variation of ω_n with respect to its nominal value. Usually, this function is expressed as a percentage—called for this reason *percent residual vibration* (PRV)—to quantify the robustness of the filter [18]. In Fig. 4(a), the PRVs of the sinusoidal smoother $S_i(s)$ and of rectangular smoother $M_i(s)$ are compared. It is evident that the sinusoidal filter (black line) outperforms the rectangular filter (red line) since the PRV is considerably smaller over the entire range of frequencies. On the other hand, it is worth noting that the value of T_i, which determines the time length of the impulse response of the smoothers, is rather different in the two cases, being $T_1 = \hat{T}_0$ for the rectangular filter and $T_1 = 1.5\hat{T}_0$ for the sinusoidal one (+50%). To perform a fair analysis, the harmonic filter $S_1(s)$ is therefore compared with a chain of two rectangular smoothers $M_1(s)M_2(s)$ (blue line), with $T_1 = \hat{T}_0$ and $T_2 = 0.5\hat{T}_0$, in order to match the time durations of the impulse response. Also, in this case, the sinusoidal filter $S_1(s)$ is more robust than the chain $M_1(s)M_2(s)$ with respect to resonance frequency variations since its PRV profile is smaller over the entire range of

This article has been accepted for inclusion in a future issue of this journal. Content is final as presented, with the exception of pagination.

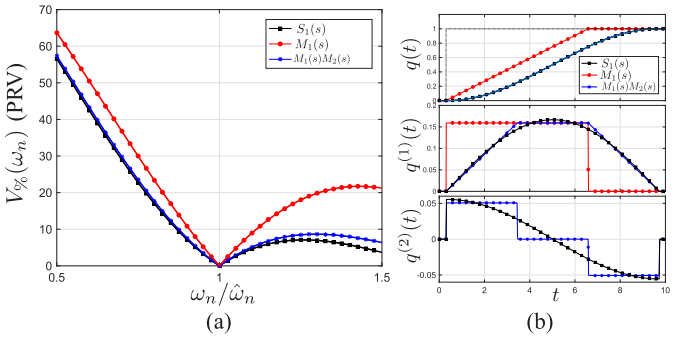

(a) (b)

Fig. 4. (a) PRV of sinusoidal and rectangular filters as a function of the normalized frequency $\omega_n/\hat{\omega}_n$. (b) Position, velocity, and acceleration profiles obtained by applying a unit step input to a sinusoidal filter $S_1(s)$ with $T_1 = 3\pi$ s and to a chain of rectangular filters $M_1(s)M_2(s)$ with $T_1 = 2\pi$ s and $T_2 = \pi$ s (b).

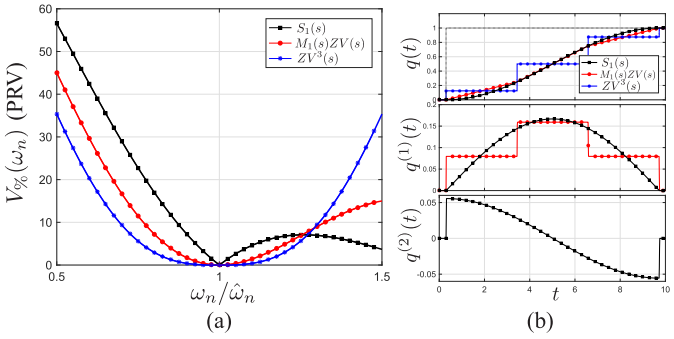

(a) (b)

Fig. 5. (a) PRV of a sinusoidal smoother compared with the combination of a rectangular smoother and a ZV input shaper and with a ZVDD input shaper. (b) Position, velocity, and acceleration profiles obtained by applying a unit step input to the three types of filters with the same total duration, i.e., $T_{tot} = 3\pi$ s.

ω_n and especially for high frequencies. Therefore, while for the compliance with kinematic constraints, two rectangular filters are preferable, for vibrations suppression, the harmonic smoother is the best option in terms of robustness.

By observing the trajectory profiles obtained by applying a simple step input to the two kinds of filters, as shown in Fig. 4(b), it results that both output trajectories have continuous velocity and limited acceleration, but their maximum values are slightly higher in the case of the harmonic motion.

Going forward, taking into account input shapers [12], the sinusoidal smoother is compared with different feedforward techniques for vibration suppression that are characterized by the same time duration, namely the combination of a rectangular filter with $T_1 = \hat{T}_0$ and a zero vibration input shaper $ZV(s)$ [19] with time constant $T_{\text{ZV}} = 0.5\hat{T}_0$ and a third-order input shaper $ZV^3(s)$ with $T_{\text{ZV}} = 0.5\hat{T}_0$, also known as zero vibration double derivative (or ZVDD) input shaper [19]. As shown in Fig. 5(b), the PRV profiles of the filters that include an input shaper are considerably lower than the PRV obtained with the sinusoidal smoother, at least in the neighborhood of $\hat{\omega}_n$. However, the filter $S_1(s)$ possesses two features that can make it preferable in many applications as follows.

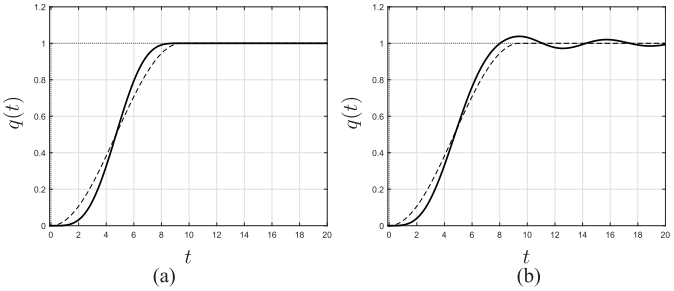

(a) (b)

Fig. 6. Response of a resonant system (solid line) with (a) $\delta = 0$ and (b) $\delta = 0.1$ to the reference trajectory $q_h(t)$ (dashed line) obtained with a sinusoidal filter $S_1(s)$ applied to a step input.

1) The PRV of the sinusoidal smoother has a low-pass characteristic, and as a consequence, the effects of additional resonant modes that may affect the plant at higher frequencies are better mitigated.
2) As already mentioned, when fed with a step signal, the trajectory produced by $S_1(s)$ is of class $\mathcal{C}^1$ (with limited acceleration), while the output of the combination $M_1(s) + ZV(s)$ is a signal of class $\mathcal{C}^0$, and the response of $ZV^3(s)$ remains of class $\mathcal{C}^{-1}$ and therefore discontinuous [see Fig. 5(b)].

V. Damped Sinusoidal Filter

If damping δ of the oscillating plant is not negligible, the filter $S_i(s)$ is unable to suppress the residual vibration even in the nominal conditions. In fact, when a step input filtered by $S_1(s)$ is applied to the system in Fig. 3, the tracking error between the load position and the motor position can be computed as

$$E(s) = \frac{-s^2}{s^2 + 2\delta\omega_n s + \omega_n^2} \cdot S_1(s) \cdot \frac{1}{s}. \tag{9}$$

By inverse Laplace transforming $E(s)$ and assuming $t \geq T_1$, the analytic expression of residual vibrations descends

$$\begin{aligned}\varepsilon(t) = {} & Ae^{-\delta\omega_n t} \\ & \times \left[\left(\omega_n^2 - \frac{\pi^2}{T_1^2} \right) (\cos(\Omega t) + e^{\delta\omega_n T_1} \cos(\Omega(t - T_1))) \right. \\ & + \frac{\delta}{\sqrt{1-\delta^2}} \left(\omega_n^2 + \frac{\pi^2}{T_1^2} \right) \\ & \left. \times (\sin(\Omega t) + e^{\delta\omega_n T_1} \sin(\Omega(t - T_1))) \right]\end{aligned}$$

where A is a constant depending on T_1, ω_n, and δ and $\Omega = \omega_n\sqrt{1-\delta^2}$. From the analytical expression of $\varepsilon(t)$, it is clear that, even if it is assumed $T_1 = 3(\pi/\Omega)$ because of the presence of $e^{\delta\omega_n T_1}$, the two terms $\cos(\Omega t) + e^{\delta\omega_n T_1} \cos(\Omega(t - T_1)$ and $\sin(\Omega t) + e^{\delta\omega_n T_1} \sin(\Omega(t - T_1))$ are not null if $\delta \neq 0$, and therefore, the residual vibration is reduced but not suppressed. In Fig. 6, the residual vibrations produced by resonant systems with $\delta = 0$ and $\delta = 0.1$, respectively, tracking a properly tuned harmonic trajectory $q_h(t)$, are compared in order to highlight this behavior.

This article has been accepted for inclusion in a future issue of this journal. Content is final as presented, with the exception of pagination.

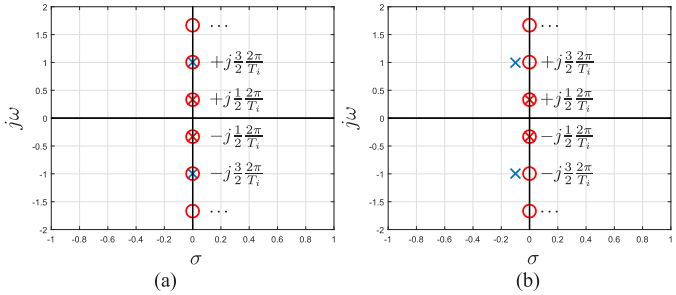

Fig. 7. Pole-zero map of $S_1(s)G_\varepsilon(s)$ for (a) $\delta = 0$ and (b) $\delta \neq 0$. In the latter case, $\sigma = -0.1$ s^{-1} ($\delta = 0.1$ and $\omega_n = 1$ rad/s).

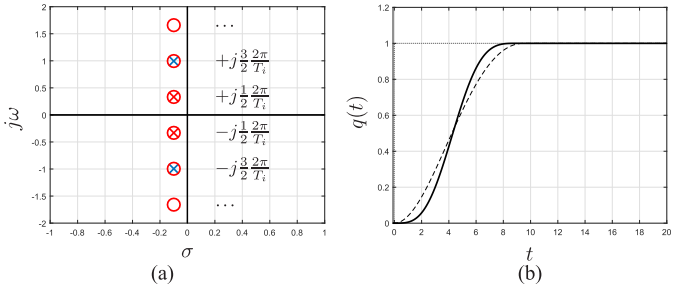

Fig. 8. Pole-zero map of the cascade $S_{\sigma,1}(s)G_\varepsilon(s)$ for (a) $\delta = 0.1$ and (b) corresponding step response.

The impossibility of canceling residual vibration with a sinusoidal filter if applied to a damped system has a straightforward explanation by analyzing the function $S_1(s)G_\varepsilon(s)$ in the S-plane. As a matter of fact, the filter $S_1(s)$ introduces an infinite number of zeros $z_k = \pm j(2k+1)(\pi/T_1)$ located along the imaginary axis. The first pair of zeros is canceled by the poles of the filter itself $p = \pm j(\pi/T_1)$, while the remaining ones can be used to cancel the oscillating poles of the plant in order to suppress the vibrations. As shown in Fig. 7(a), if $\delta = 0$, a perfect cancelation occurs since also the poles of the plant lie on the imaginary axis. Conversely, if $\delta \neq 0$, this cancelation does not take place [see Fig. 7(b)], and the zeroing effect, which is responsible for the vibration reduction, decreases as the oscillating mode moves away from the imaginary axis, that is as δ grows. In order to obtain a perfect cancelation even for damped plants, a possible solution consists of translating zeros (and poles) of $S_1(s)$ along a line parallel to the imaginary axis whose abscissa is equal to the real part of the poles of $G_\varepsilon(s)$. The procedure used in [20] for rectangular filters, based on a frequency shift of the real quantity σ_i and on a modification of the gain in order to assure unitary static gain, has been followed, and the transfer function of the new smoother has been derived:

$$S_{\sigma,i}(s) = k\, S_i(s-\sigma_i) = \frac{\left(\frac{\pi}{T_i}\right)^2 + \sigma_i^2}{1 + e^{\sigma_i T_i}} \frac{1 + e^{-sT_i} e^{\sigma_i T_i}}{(s-\sigma_i)^2 + \left(\frac{\pi}{T_i}\right)^2}. \tag{10}$$

By defining

$$\sigma_i = -\delta\omega_n \quad \text{and} \quad T_i = \frac{3\pi}{\omega_n\sqrt{1-\delta^2}} \tag{11}$$

a perfect cancelation of the damped poles of the plant is achieved by the zeros of $S_{\sigma,i}(s)$ [see Fig. 8(a)]. As a consequence, the application to the system of a trajectory, generated by feeding the filter with a step input, does not cause residual vibrations, as highlighted in Fig. 8(b). From an analytical point of view, the expression of residual vibrations considering a damped sinusoidal smoother $S_{\sigma,1}(s)$ filtering a step input becomes

$$\begin{aligned}\varepsilon(t) = Ae^{-\delta\omega_n t}[B(\cos(\Omega t) + e^{(\sigma_1+\delta\omega_n)T_1}\cos(\Omega(t-T_1))) \\ + C(\sin(\Omega t) + e^{(\sigma_1+\delta\omega_n)T_1}\sin(\Omega(t-T_1)))]\end{aligned} \tag{12}$$

where $\Omega = \omega_n\sqrt{1-\delta^2}$, and A, B, and C are the constant parameters that depend on σ_1, T_1, δ, and ω_n. Therefore, the necessary and sufficient condition that guarantees $\varepsilon(t) = 0$, $\forall t \geq T_1$, is

$$\sigma_1 = -\delta\omega_n \quad \text{and} \quad T_1 = k\frac{3\pi}{\omega_n\sqrt{1-\delta^2}}, \quad k = 1, 2, \ldots \tag{13}$$

Note that the condition (11) is a particular case of (13), leading to the minimum duration of the trajectory.

By inverse Laplace transforming $S_{\sigma,i}(s)$, its impulse response is obtained, i.e.,

$$s_{\sigma,i}(t) = \begin{cases} \dfrac{\left(\frac{\pi}{T_i}\right)^2 + \sigma_i^2}{1 + e^{\sigma_i T_i}} \dfrac{T_i}{\pi} e^{\sigma_i t} \sin\left(\dfrac{\pi}{T_i}t\right), & 0 \leq t \leq T_i \\ 0, & \text{otherwise.} \end{cases} \tag{14}$$

Since $s_{\sigma,i}(t)$ is given by the product of a sine function and an exponential function with $\sigma_i < 0$ (the plant is supposed to be asymptotically stable), $S_{\sigma,i}(s)$ is called the *damped sinusoidal filter*. When fed with a step input, it provides a *damped harmonic trajectory*, which generalizes the standard harmonic motion and whose analytical expression is

$$\begin{aligned}q_{h,\sigma}(t) = q_0 + \frac{h}{1 + e^{\sigma_1 T_1}}\Big(1 + e^{\sigma_1 t}\Big(\frac{\sigma_1 T_1}{\pi}\sin\Big(\frac{\pi}{T_1}t\Big) \\ - \cos\Big(\frac{\pi}{T_1}t\Big)\Big)\Big)\end{aligned}$$

where q_0 is the initial position, h is the desired displacement, T_1 is the duration of the trajectory, and σ_1 is the decay rate coefficient. Note that the impulse response of the filter $s_{\sigma,i}(t)$ coincides with the velocity of the damped harmonic trajectory. In Fig. 9, the shape of $s_{\sigma,i}(t)$ for different values of σ_i is shown, and it is possible to appreciate that $s_{\sigma,i}(t)$ becomes more and more asymmetric, as the magnitude of σ_i grows and its peak value tends to increase as well. This means that, for a given value of T_i, the velocity of the damped harmonic motion, i.e., the first derivative of the filter step response, grows with $|\sigma_i|$.

A. Parameter Identification and Sensitivity to Errors

The filter parameters σ_i and T_i can be readily determined by applying (13) once the nominal values of the damping coefficient $\hat{\delta}$ and of natural frequency $\hat{\omega}_n$ of the resonant plant are known. Alternatively, as for the other smoothing filters or input shapers, it is possible to experimentally estimate their values. As a matter of fact, condition (13) that assures

This article has been accepted for inclusion in a future issue of this journal. Content is final as presented, with the exception of pagination.

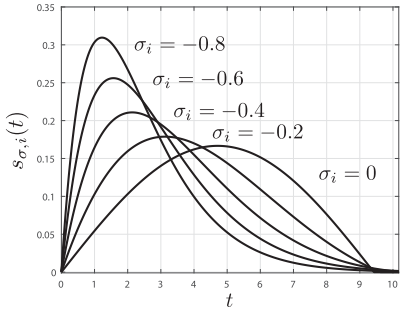

Fig. 9. Impulse response $s_{\sigma,i}(t)$ of the damped harmonic smoother for different values of σ_i.

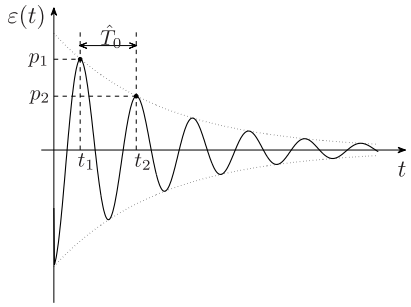

Fig. 10. Residual vibrations caused by the applications of a step input to the resonant system shown in Fig. 3.

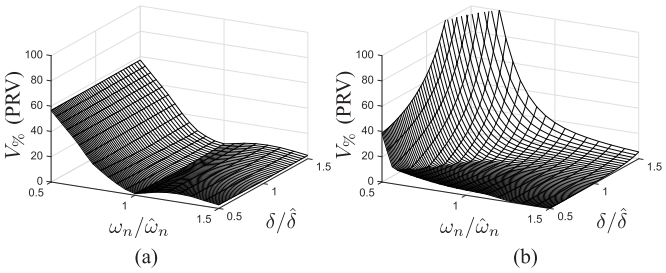

Fig. 11. PRV of $S_{\sigma,i}(s)$ as a function of ω_n and δ normalized with respect to their nominal values for (a) $\hat{\delta} = 0.05$ and (b) $\hat{\delta} = 0.5$.

residual vibration suppression for the second-order system with poles $p_{1,2} = \hat{\sigma} \pm j\hat{\Omega} = -\hat{\delta}\hat{\omega}_n \pm j\hat{\omega}_n\sqrt{1-\hat{\delta}^2}$ can be rewritten as

$$\sigma_i = -\hat{\delta}\hat{\omega}_n = \hat{\sigma}\,, \quad T_i = k\frac{3\pi}{\hat{\Omega}} = k\frac{3}{2}\hat{T}_0, \quad k = 1, 2, \ldots \tag{15}$$

As a consequence, the two parameters can be obtained by analyzing the vibrations induced on the plant by a generic input signal or nonnull initial conditions, vibrations characterized by a period $\hat{T}_0 = (2\pi/\hat{\Omega})$ and an exponential decay rate $\hat{\sigma}$. With reference to Fig. 10, their numerical values are

$$\begin{aligned} T_i &= \frac{3}{2}\hat{T}_0 \quad \text{with } \hat{T}_0 = t_2 - t_1 \\ \sigma_i &= \frac{1}{\hat{T}_0}\ln\left(\frac{p_2}{p_1}\right) \end{aligned} \tag{16}$$

where the parameters t_1, t_2, p_1, and p_2 are defined. For more details, see [20].

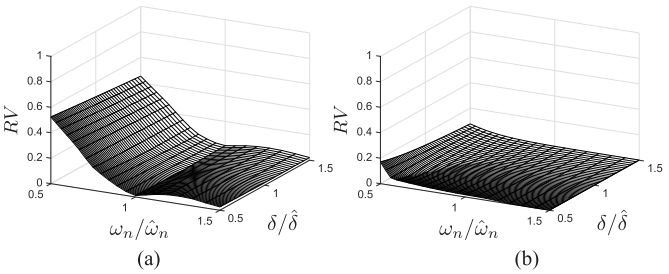

Fig. 12. Maximum magnitude of the residual vibration caused by $S_{\sigma,i}(s)$ fed with a unit step input as a function ω_n and δ normalized with respect to their nominal values for (a) $\hat{\delta} = 0.05$ and (b) $\hat{\delta} = 0.5$.

As for the undamped sinusoidal filter, the choice of the parameters of $S_{\sigma,i}(s)$ is critical to the level of residual vibration, but in this case, there are two independent variables. For this reason, the 3-D surface describing the PRV as a function of δ and ω_n has been computed. In particular, since the PRV of $S_{\sigma,i}(s)$ depends on the nominal value of the plant damping coefficient $\hat{\delta}$, two different values have been considered in order to analyze the performance of the filter for small ($\hat{\delta} = 0.05$) and large ($\hat{\delta} = 0.5$) damping values. Conversely, the nominal value of the natural frequency does not affect the PRV, and therefore, a generic value $\hat{\omega}_n$ has been assumed. In Fig. 11, the two surfaces are shown. For small values of $\hat{\delta}$, see Fig. 11(a), the PRV of the filter strongly depends on the correct estimation of ω_n, while it is practically not sensitive to errors on δ. On the other hand, for large values of $\hat{\delta}$, both parameters may be critical, and it seems that for $\omega_n \ll \hat{\omega}_n$ and $\delta \gg \hat{\delta}$, the presence of the filter $S_{\sigma,i}(s)$ increases the level of vibrations. However, it is worth noting that in this case, the apparent high level of residual vibrations is due to the definition of PRV as the ratio between the maximum amplitude of vibrations with and without a filter. Since the vibrations for large values of $\hat{\delta}$ are very small, the denominator of the function for the computation of PRV is small as well and may lead to large values even if the numerator is limited. These considerations are very clear if the absolute value of the residual vibration (with a unit step input) is considered in place of the percentage, as in Fig. 12. If $\hat{\delta}$ is small, the contribution of the filter is very important, and accordingly, the estimation of the parameters is a critical issue, while for larger values of $\hat{\delta}$, the role played by $S_{\sigma,i}(s)$ is less significant since, in any case, the level of the vibration is very limited [see Fig. 12(b)].

Similar to the undamped case, the results obtained with the filter $S_{\sigma,i}(s)$, in terms of PRV, are compared with those produced by a chain of two exponential filters $M_{\sigma,1}(s)M_{\sigma,2}(s)$, which represent the generalization of the rectangular smoothers $M_1(s)M_2(s)$ to consider the damping coefficient of the plant [20] (see Fig. 13). The (damped) sinusoidal smoother continues to outperform the chain of "rectangular" filters since the PRV value is smaller.

Finally, since the two characteristic parameters of $S_{\sigma,i}(s)$ are often directly obtained, it is worth considering the sensitivity of the filter with respect to errors on T_i and σ_i, as in Fig. 14. In this case, even considering two different values of $\hat{\delta}$, the conclusion is quite straightforward: errors on σ_i have a

This article has been accepted for inclusion in a future issue of this journal. Content is final as presented, with the exception of pagination.

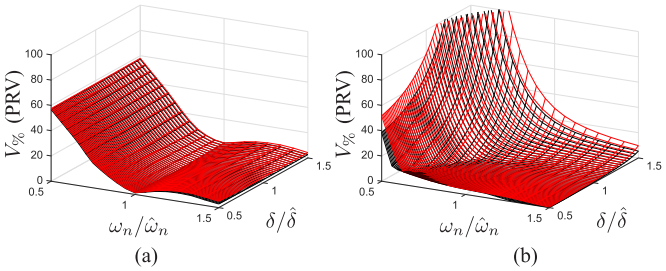

Fig. 13. PRV of $M_{\sigma,1}(s)M_{\sigma,2}(s)$ (red line surface) compared with $S_{\sigma,i}(s)$ (black line surface) as a function of ω_n and δ normalized with respect to their nominal values for (a) $\hat{\delta} = 0.05$ and (b) $\hat{\delta} = 0.5$.

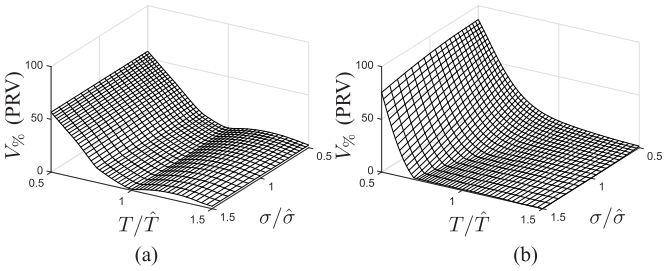

Fig. 14. PRV of $S_{\sigma,i}(s)$ as a function of the impulse length T_i and decay rate σ_i, normalized with respect to their nominal values, for (a) $\hat{\delta} = 0.05$ and (b) $\hat{\delta} = 0.5$.

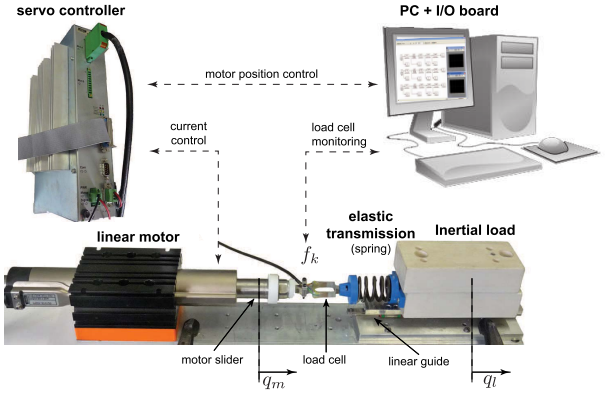

Fig. 15. Experimental setup.

little influence on the PRV, while the estimation of T_i is very critical for an effective vibration reduction.

VI. Comparative Experimental Evaluation of the Damped Sinusoidal Filter

In order to experimentally test the proposed method, the setup shown in Fig. 15 has been arranged. It is composed of a linear motor, LinMot PS01-37x120, whose slider is connected to an inertial load by means an elastic transmission obtained with a coil spring. The setup can be modeled as an ideal two-mass system with the elastic transmission, characterized by the second-order oscillatory dynamics as the one reported in Fig. 3. The control system is based on the servo controller LinMot E2010-VF that performs the basic current control, while the position control (based on a proportional–integral–differential controller and a feedforward action) has been implemented on a standard PC with a Pentium IV 3-GHz processor equipped with a Sensoray 626 I/O board, used to both communicate with the servo controller and acquire the sensors signals. The real-time operating system RTAI-Linux allows the position controller to run with a sampling period $T_s = 500\ \mu$s. Obviously, a digital implementation of all the filters tested in the experiments has been used. For the damped harmonic smoother, the expression of the discrete-time transfer function, obtained by Z-transforming (10) and imposing a unitary static gain, is

$$S_{\sigma,i}(z^{-1}) = K_i \frac{z^{-1} + e^{\sigma_i N_i T_s} z^{-(N_i+1)}}{1 - 2e^{\sigma_i T_s}\cos\left(\frac{\pi}{N_i}\right)z^{-1} + e^{2\sigma_i T_s} z^{-2}} \qquad (17)$$

where

$$K_i = \frac{1 - 2e^{\sigma_i T_s}\cos\left(\frac{\pi}{N_i}\right) + e^{2\sigma_i T_s}}{1 + e^{\sigma_i N_i T_s}}$$

and $N_i = \text{round}(T_i/T_s)$.

In order to evaluate the residual vibrations ε, a load cell is placed between the slider and the elastic transmission. As a matter of fact, the force f_k exerted by the spring is related to the error between the motor and the load position, and if the inherent damping of the transmission is considered, the force f_k is simply a scaled low-pass filtered version of ε.

The parameters of the plant have been identified according to the procedure reported in Section V-A, by applying to the motor the trapezoidal velocity trajectory of Fig. 16 and analyzing the response of the system, in terms of force $f_k(t)$ transmitted via the coil spring. The poles, $p_{1,2} = \hat{\sigma} \pm j\hat{\Omega}$, of the second-order system are characterized by

$$\hat{\sigma} = -15.6539\ \text{1/s} \quad \text{and} \quad \hat{\Omega} = 122.7185\ \text{rad/s}$$

and, consequently, $\hat{T}_0 = (2\pi/\hat{\Omega}) = 0.0512$ s. The values of $\hat{\sigma}$ and $\hat{T}_0$ have been used for designing the damped sinusoidal smoother and the other filtering methods mentioned in Section IV in order to make a comparative analysis. The reference trajectories obtained by filtering a step input of amplitude 30 mm and the corresponding profiles of the force $f_k(t)$ induced on the plant are reported in Fig. 17. By observing the column on the right, that shows the vibration at the end of the motion, the experimental results confirm the theoretical analysis discussed in Sections IV and V. First of all, the comparison of Fig. 17(e) and (d) highlights that the damped sinusoidal filter $S_{\sigma,1}(s)$ outperforms the standard sinusoidal filter $S_1(s)$ in terms of residual vibration level and produces a response that is very similar to the cascade of two exponential smoothers $M_{\sigma,1}(s)M_{\sigma,2}(s)$ shown in Fig. 17(a). The peak values of the

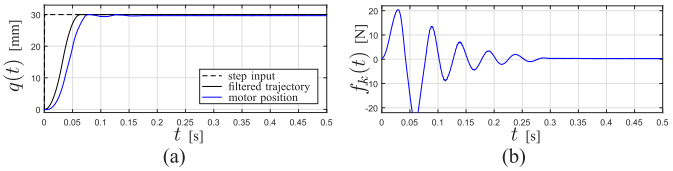

Fig. 16. Response of the two-mass system of Fig. 15 to a trapezoidal velocity trajectory of duration (a) $T_{tot} = 0.0635$ s and (b) residual vibrations.

This article has been accepted for inclusion in a future issue of this journal. Content is final as presented, with the exception of pagination.

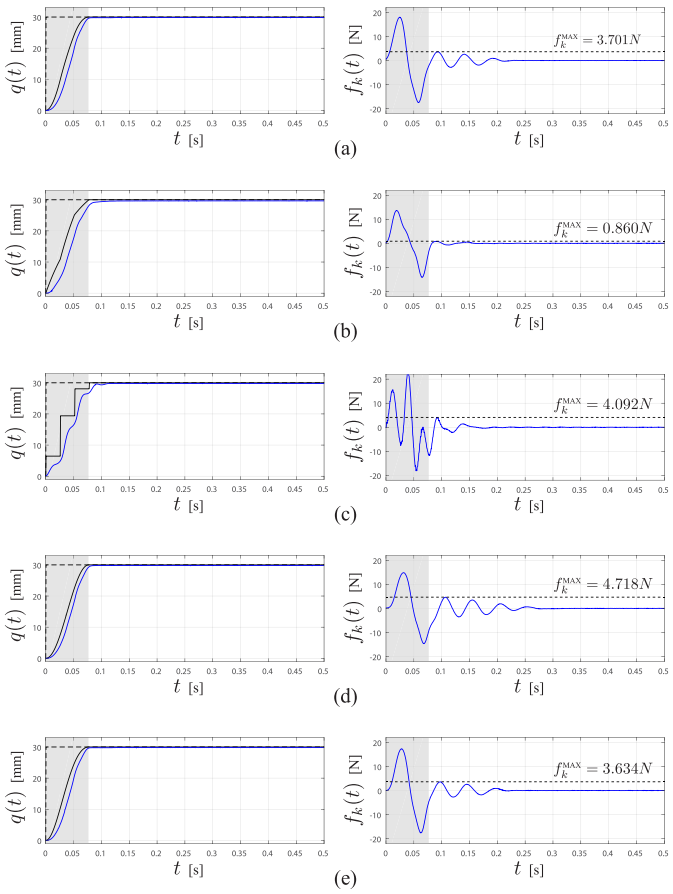

Fig. 17. Response of the two-mass system of Fig. 15 and residual vibration induced by several motion profiles obtained by filtering a step signal. Left: resulting trajectory $q(t)$. Right: transmission force $f_k(t)$ proportional to ε. (a) Exponential^2 $M_{\sigma,1}(s)M_{\sigma,2}(s)$. (b) Exponential + ZV is $M_{\sigma,1}(s)ZV(s)$. (c) ZVDD is $ZV^3(s)$. (d) Sinusoidal $S_1(s)$. (e) Damped sinusoidal $S_{\sigma,1}(s)$.

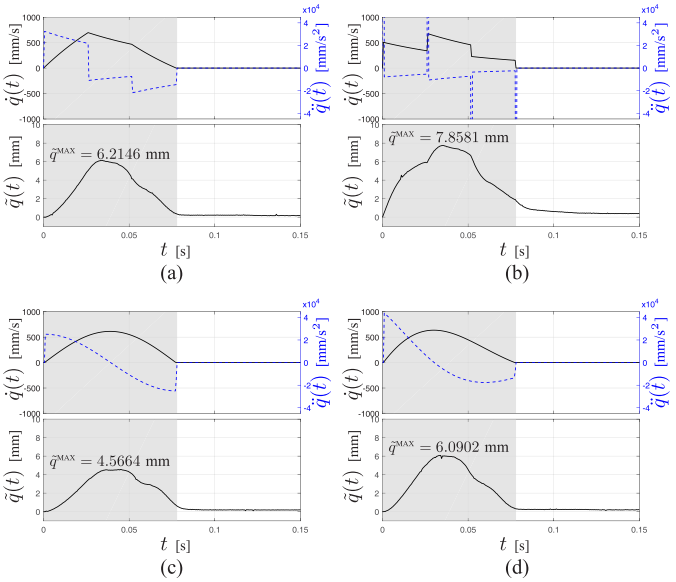

Fig. 18. Velocity and acceleration of the motion profiles obtained with different filters and tracking error $\tilde{q}(t)$ of the motor. (a) $M_{\sigma,1}(s)M_{\sigma,2}(s)$. (b) $M_{\sigma,1}(s)ZV(s)$. (c) $S_1(s)$. (d) $S_{\sigma,1}(s)$.

residual vibration, measured via the transmission force, are 3.634 and 4.718 N for $S_{\sigma,1}(s)$ and $S_1(s)$, respectively, while $f_k^{\text{MAX}} = 3.701$ N for $M_{\sigma,1}(s)M_{\sigma,2}(s)$. The use of input shapers may enhance the vibration reduction but only if they are used in conjunction with the smoothers filters. In fact, despite the fact that, according to the sensitivity function reported in Fig. 5, the ZVDD input shapers are accounted for as the most robust filtering method with respect to errors in the parameters estimation, it produces a very high level of oscillations ($f_k^{\text{MAX}} = 4.092$ N) and, in particular, greater than the level obtained by sinusoidal filters. This result can be ascribed to the large tracking error of the linear motor that is very fast but cannot follow discontinuous steps [see Fig. 17(c) (left)]. On the contrary, the combination $M_{\sigma,1}(s)ZV(s)$ generates a level of the residual vibration smaller than the one produced by the other filtering methods involving the same time delay. Therefore, if the goal of the filter only consists of the residual vibration suppression, the combination $M_{\sigma,1}(s)ZV(s)$ is the optimal choice. However, if other features of the resulting motion trajectories, such as smoothness level, velocity/acceleration peak values, and tracking error, are considered, different filters should be preferred. In Fig. 18, it is shown that the filter $M_{\sigma,1}(s)ZV(s)$ fed with a step input produces a motion profile characterized by discontinuous velocity and, consequently, infinite acceleration. Correspondingly, the tracking error $\tilde{q}(t) = q_{\text{ref}}(t) - q_m(t)$ between the desired and actual motion profiles of the motor has the largest value ($\tilde{q}^{\text{MAX}} = 7.8581$ mm) among all the tested trajectory filters (in this case, the ZVDD input shaper is not considered because it is not a trajectory filter). On the contrary, the trajectory of class $\mathcal{C}^1$ produced by the (undamped) sinusoidal smoother $S_1(s)$ exhibits the smallest velocity and acceleration values and the smallest tracking error ($\tilde{q}^{\text{MAX}} = 4.5664$ mm). The damped harmonic smoother $S_{\sigma,1}(s)$ and the cascade of two exponential smoothers $M_{\sigma,1}(s)M_{\sigma,2}(s)$ lead to similar performances, with a slight superiority of $S_{\sigma,1}(s)$, which is characterized by a lower velocity and a smaller tracking error ($\tilde{q}^{\text{MAX}} = 6.0902$ mm).

VII. Conclusion

The aim of this brief is to prove advantages and disadvantages of trajectories based on the trigonometric functions, starting from the initial consideration that this kind of motion profiles can be obtained by a cascade of smoothers with the rectangular and sinusoidal impulse response. After having remarked that in those applications that involve only kinematic constraints, the use of harmonic smoothers is useless, since, for given bounds, a cascade of two rectangular smoothers leads to trajectories with the same continuity level but lower duration, it has been shown, with both theoretical considerations and experimental tests, that harmonic smoothers are preferable for vibration suppression. In this respect, the generalization of the harmonic smoother to consider not only the natural frequency but also the damping coefficient of the vibrating plant appears a significant improvement. The damped harmonic smoother further enhances the capability of the harmonic smoother of

This article has been accepted for inclusion in a future issue of this journal. Content is final as presented, with the exception of pagination.

reducing the residual vibration without a significant increase of the complexity.

REFERENCES

[1] R. Nozawa, H. Kawamura, and T. Sasaki, "Acceleration/deceleration circuit," U.S. Patent 4 554 497 A, Nov. 19, 1985.

[2] D.-I. Kim, J. W. Jeon, and S. Kim, "Software acceleration/deceleration methods for industrial robots and CNC machine tools," *Mechatronics*, vol. 4, no. 1, pp. 37–53, Feb. 1994.

[3] J. W. Jeon and Y. Y. Ha, "A generalized approach for the acceleration and deceleration of industrial robots and CNC machine tools," *IEEE Trans. Ind. Electron.*, vol. 74, no. 1, pp. 133–139, Feb. 2000.

[4] R. Zanasi, C. G. Lo Bianco, and A. Tonielli, "Nonlinear filters for the generation of smooth trajectories," *Automatica*, vol. 36, no. 3, pp. 439–448, 2000.

[5] C. Zheng, Y. Su, and P. Müller, "Simple online smooth trajectory generations for industrial systems," *Mechatronics*, vol. 19, no. 4, pp. 571–576, 2009.

[6] L. Biagiotti and R. Zanasi, "Time-optimal regulation of a chain of integrators with saturated input and internal variables: An application to trajectory planning," *IFAC Proc. Vol.*, vol. 43, no. 14, pp. 1278–1283, 2010.

[7] C. G. Lo Bianco and F. Ghilardelli, "A discrete-time filter for the generation of signals with asymmetric and variable bounds on velocity, acceleration, and jerk," *IEEE Trans. Ind. Electron.*, vol. 61, no. 8, pp. 4115–4125, Aug. 2014.

[8] L. Biagiotti and C. Melchiorri, "FIR filters for online trajectory planning with time- and frequency-domain specifications," *Control Eng. Pract.*, vol. 20, no. 12, pp. 1385–1399, 2012.

[9] H. Li, Z. Gong, W. Lin, and T. Lippa, "Motion profile planning for reduced jerk and vibration residuals," Singapore Inst. Manuf. Technol., Singapore, Tech. Rep. 8, Jan./Mar. 2007.

[10] R. Bearee, P.-J. Barre, and J.-P. Hautier, "Vibration reduction abilities of some jerk-controlled movement laws for industrial machines," *IFAC Proc. Vol.*, vol. 38, no. 1, pp. 796–801, 2005.

[11] T. Singh, "Jerk limited input shapers," *J. Dyn. Syst., Meas., Control*, vol. 126, no. 1, pp. 215–219, Apr. 2004.

[12] W. Singhose, R. Eloundou, and J. Lawrence, "Command generation for flexible systems by input shaping and command smoothing," *J. Guid., Control, Dyn.*, vol. 33, no. 6, pp. 1697–1707, 2010.

[13] T. Vyhlídal and M. Hromvcík, "Parameterization of input shapers with delays of various distribution," *Automatica*, vol. 59, pp. 256–263, Sep. 2015.

[14] B. Alikocc, T. Vyhlídal, and A. F. Ergencc, "Closed-form smoothers and shapers with distributed delay for damped oscillatory modes," *IET Control Theory Appl.*, vol. 10, no. 18, pp. 2534–2542, Dec. 2016.

[15] L. Biagiotti and C. Melchiorri, "Online planning of multi-segment trajectories with trigonometric blends," *IFAC Proc. Vol.*, vol. 44, no. 1, pp. 10343–10348, 2011.

[16] L. Moriello, L. Biagiotti, and C. Melchiorri, "Multidimensional trajectories generation with vibration suppression capabilities: The role of exponential B-splines," *IFAC-PapersOnLine*, vol. 50, no. 1, pp. 6054–6059, 2017.

[17] N. Singer, W. Singhose, and W. Seering, "Comparison of filtering methods for reducing residual vibration," *Eur. J. Control*, vol. 5, nos. 2–4, pp. 208–218, 1999.

[18] K. Kozak, W. Singhose, and I. Ebert-Uphoff, "Performance measures for input shaping and command generation," *J. Dyn. Syst., Meas., Control*, vol. 128, no. 3, pp. 731–736, 2006.

[19] N. C. Singer and W. P. Seering, "Preshaping command inputs to reduce system vibration," *ASME J. Dyn. Syst., Meas., Control*, vol. 112, no. 1, pp. 76–82, 1990.

[20] L. Biagiotti, C. Melchiorri, and L. Moriello, "Optimal trajectories for vibration reduction based on exponential filters," *IEEE Trans. Control Syst. Technol.*, vol. 24, no. 2, pp. 609–622, Mar. 2016.